Machine Learning-Based Classification of Catheter Ablation Site Using Person-Sensitive CARTO Coordinate Data

Naoki Tomizawa
Facility of data science
Musashino University
Tokyo, Japan
g2350004@stu.musashino-u.ac.jp

Virach SORNLERTLAMVANICH
Facility of data science
Musashino University
Tokyo, Japan
httpss://orcid.org/0000-0002-6918-8713

Thatsanee CHAROENPORN
Facility of data science
Musashino University
Tokyo, Japan
https://orcid.org/0000-0002-9577-9082

Abstract— **The world's population is growing, posing challenges in an aging society. As we anticipate a rise in atrial fibrillation (AF) with aging, there is a growing demand for efficient treatment methods. In this research, our goal is to partially automate the operation of 3D mapping systems used in AF treatment with the CARTO system. We analyze the X, Y, and Z coordinate axes data labeled LPV, RPV, and CTI extracted from the CARTO system. The analysis includes both a single-case dataset and a mixed dataset of 10 cases. Initially, we visualize the data using principal component analysis. Subsequently, we compare the classification accuracy of different classifiers—k-Nearest Neighbors, Gaussian Mixture Model, SGD Classification, and Linear SVC. While all models achieve 1.0 accuracy in the single-case dataset, the highest accuracy score in the mixed dataset of 10 cases is 0.982, obtained by k-Nearest Neighbors.**

Keywords-Atrial fibrillation; CARTO; Machine learning; Atifical intilligence; Catheter Ablation

I. Introduction

The world's population has experienced dramatic growth in both size and the proportion of elderly individuals. Estimated to be 8.0 billion in mid-November 2022, the global population is projected to increase to 9.7 billion in the 2050s and nearly 10.4 billion in the mid-2080s [1]. Even more, the median age of the world's population will be going to increase from 26.6 years in 2000 to 37.3 years in 2050 and then to 45.6 years in 2100 [2]. By 2030, one in six people worldwide will be aged 60 years or over, and this number is expected to double, reaching 2.1 billion by the 2050s. The imminent arrival of a super-aging society on a global scale is certain in the very near future. The aging society will undoubtedly bring about various challenges, particularly in maximizing the health and well-being of the elderly, ensuring non-discrimination in health and social care, and researching treatments with the lowest risk and highest efficiency.

Cerebral artery disease, commonly known as stroke, stands as a prevalent cause of mortality among the elderly, ranking closely behind ischemic heart disease. A crucial factor contributing to this disease, leading to blood vessel blockage, is atrial fibrillation (AF). Particularly prominent in the elderly population, AF poses a substantial risk of cardiogenic ischemic stroke. Despite the global prevalence of AF being less than 1%, its incidence rises significantly among individuals aged 80 years and above, reaching approximately 7–14% in Western countries and 2–3% in Japan. Complications from AF treatment see a notable increase in patients aged 75 years and over. Consequently, the ongoing demographic shift in the global aging population is expected to result in a surge of AF cases, affecting an estimated 5–16 million people in the United States and over 1 million in Japan by 2050 [3]. This demographic transition underscores the continuing imperative for effective and efficient strategies and methodologies in therapeutic and caregiving practices for this growing patient demographic.

AF, or atrial fibrillation, is a form of irregular heartbeat, or arrhythmia, characterized by irregular and chaotic contractions in the upper chambers of the heart known as the atria. Normally, the atria work in a coordinated manner to pump blood to the lower chambers, or ventricles. However, in the case of AF, the electrical signals within the atria become disorganized, leading to quivering or fibrillation instead of the usual coordinated contractions [4]. This irregular heartbeat can manifest various symptoms, including the heightened risk of stroke, as mentioned earlier. To address AF, doctors often employ radiofrequency during treatment procedures to electrically isolate the affected veins [5]. This involves inserting a catheter into the heart, a process that demands careful attention to the catheter's position. In undertaking AF treatment, the use of fluoroscopy equipment and 3-dimensional mapping systems is common. These technologies are employed strategically to mitigate the potential harmful effects of radiation on the human body, emphasizing the importance of precision and safety in these medical interventions.

The widely adopted medical 3D imaging technology on a global scale is CARTO, initially introduced by Biosense Webster, a Johnson & Johnson MedTech company, in 1996 [6]. The fundamental operation of CARTO relies on a triangular electromagnetic source generated by three distinct ultra-low magnetic fields, as depicted in Fig. 1A. This unique configuration allows for the continuous measurement of the catheter's distance from each of the three magnetic generators positioned beneath the operating table, thereby enabling precise localization of the catheter tip in three-dimensional space.

To enhance accuracy, an external patch is strategically placed on the patient's anterior and posterior thorax to detect possible unintentional movements, as illustrated in Fig. 1B. Fig. 1C provides an overview of the typical configuration of the CARTO system within the electrophysiology laboratory. This advanced technology plays a crucial role in guiding medical procedures, providing clinicians with real-time, accurate insights into the spatial dynamics of the targeted areas, ultimately contributing to improved patient outcomes.

While the use of this system is widely popular, limitations persist in terms of usage and human error. Particularly, during electrocautery procedures, a treatment team is tasked with meticulously recording the specific points or areas to be treated. This manual recording process can be time-consuming, contributing to tension among the team members and increasing the risk of errors. In response to these limitations, we have implemented machine learning algorithms to enhance the treatment flow. These interventions are designed to improve team efficiency, expedite procedures, and minimize error rates.

The main contributions of the paper includes

1) Validation of the classification models for the catheter ablation site of CARTO coordinate data.

2) Applicability of the proposed model to person-sensitive CARTO coordinate data.

3) Viability of the proposed method without device calibration.

The remaining part of this paper is structured as follows. Session II describes coordinate data classification. The application of CARTO system is introduced in Session III, with dataset of ablation site of CARTO system in Session IV. Result of experiment, conclusion and future work are in Session V and VI respectively.

II. Coordinate Data Classification

In this section, we present an in-depth analysis of the X, Y, and Z coordinate data labeled LPV, RPV, and CTI, extracted from the CARTO system. The initial step involved employing principal component analysis (PCA) to achieve dimension reduction while preserving the intrinsic value of the data. This reduction facilitated a visual examination of the dataset's characteristics.

Subsequently, a comparative analysis of prediction accuracy was conducted using four distinct classifiers: k-Nearest Neighbors (k-NN), Gaussian Mixture Model (GMM), SGD Classification (SGDClassifier), and Linear SVC (LinearSVC). To assess the robustness of these models, two distinct datasets were utilized for this comparative study: a single-case dataset and a combined dataset comprising 10 cases.

A. k-Nearest Neighbors (k-NN)

The k-NN algorithm classifies a new data point based on the majority class of its k-nearest neighbors in the training dataset [7]. Operating in a feature space, k-NN is effective for datasets with clear patterns. The parameter 'k' dictates the number of neighbors considered during predictions, with smaller 'k' values making the model sensitive to noise and larger 'k' values resulting in smoother decision boundaries. During training, distances between data points are calculated using the training dataset, and predictions are made based on the majority vote of the k-nearest neighbors.

B. Gaussian Mixture Model (GMM)

GMM, a powerful statistical tool for pattern recognition based on clustering techniques [8], was employed in this study. By representing data as a mixture of Gaussian distributions, GMM accommodates diverse patterns. Its versatility extends across various domains, including image and speech processing, clustering, and anomaly detection. This makes GMM invaluable for revealing hidden patterns within complex datasets.

C. SGC Classification (SGDClassifier)

The SGDClassifier, a linear classification algorithm utilizing Stochastic Gradient Descent (SGD) for optimization [9], was chosen for its efficiency with large-scale and sparse datasets. The algorithm iteratively updates model weights by processing one training sample at a time, making it computationally efficient for streaming data or large datasets.

D. Linear SVC (LinearSVC)

LinearSVC is a linear classification algorithm rooted in the Support Vector Machine (SVM) framework [10]. It classifies data into two or more classes using a linear decision boundary. The algorithm seeks to find a hyperplane that effectively separates classes in the feature space. The term "linear" denotes that the decision boundary is a linear combination of input features. Unlike SVC, LinearSVC employs a linear kernel by default, making it particularly suitable for datasets with linearly separable classes.

III. CARTO System

The CARTO system, a pivotal 3-dimensional mapping system, has achieved widespread adoption globally, offering crucial insights into cardiac electrophysiology. Introduced by Biosense Webster (currently Johnson & Johnson) in 1996, CARTO has become an indispensable tool for guiding complex cardiac interventions.

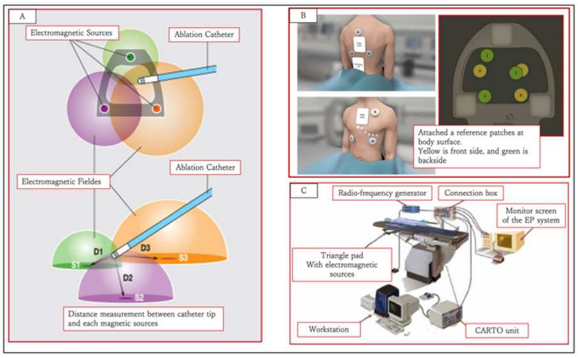

Figure 1. Basic mechanism and typical setup of the CARTO system [6].

Figs. 1A. to 1C. illustrate the fundamental mechanism, patient movement monitoring, and typical setup of the CARTO system, providing a visual guide to its advanced features and applications in cardiac electrophysiology.

A. CARTO System Mechanism

The fundamental mechanism of the CARTO system relies on a triangular electromagnetic source, utilizing three distinct ultralow magnetic fields shown in Fig. 1A. This innovative design enables the continuous measurement of the catheter's distance relative to three magnetic generators positioned beneath the operating table. As a result, the system can precisely localize the catheter tip in three-dimensional space. This real-time spatial information is pivotal for navigating the intricate anatomy of the heart during procedures.

B. Patient Movement Monitoring

To ensure accuracy and account for any unintentional patient movements, an external reference patch is strategically placed on the patient's front and back as shown in Fig. 1B. This patch serves as a reference point for the system, allowing it to detect and compensate for potential shifts in the patient's position.

C. Laboratory Setup

The typical setup of the CARTO system in the electrophysiology laboratory is illustrated in Figure 1C. This configuration showcases the integration of advanced technology to provide clinicians with a comprehensive visualization of the cardiac anatomy during procedures. The seamless synergy between the electromagnetic source, catheter localization, and patient movement monitoring contributes to the system's effectiveness in guiding catheter ablation interventions.

D. Catheter Ablation Targets

Common ablation sites for cardiac arrhythmias, such as atrial fibrillation (AF), include the left pulmonary vein (LPV), right pulmonary vein (RPV), and Cavotricuspid isthmus (CTI). These specific targets are critical areas where abnormal electrical pathways may be addressed through ablation procedures.

The primary aim of this research is to explore the feasibility of automated recognition of ablation sites within the CARTO system. This initiative seeks to demonstrate the potential for automated processes to succeed human intervention, ultimately alleviating the burden on medical staff. The integration of machine learning algorithms, as explored in this study, represents a step toward enhancing the efficiency and precision of ablation site identification during catheter-based interventions.

IV. Dataset of Ablation Site in CARTO System

In the dataset of a single case, the results of principal component analysis revealed a distinct separation of data labeled LPV, RPV, and CTI without any observed overlap, demonstrating the efficacy of the CARTO system in capturing intricate spatial patterns as shown in Fig. 2A. However, when examining the mixed dataset comprising 10 cases, a noteworthy observation emerged: the RPV data exhibited overlap with both LPV and CTI labels as shown in Fig. 2C. This phenomenon underscores the potential variability and complexity introduced when considering a broader set of patient data.

The data is converted to 2-dimensional coordinates (X, Y, Z) using principal component analysis, showcasing the robustness of the methodology in elucidating spatial relationships. In the context of a single case, the labels for LPV, RPV, and CTI maintain distinct separation as shown in Fig. 2B. Contrarily, in the mixed dataset of 10 cases, it becomes evident that the RPV label shows overlap with both LPV and CTI labels, emphasizing the importance of considering diverse patient data as shown in Fig. 2D.

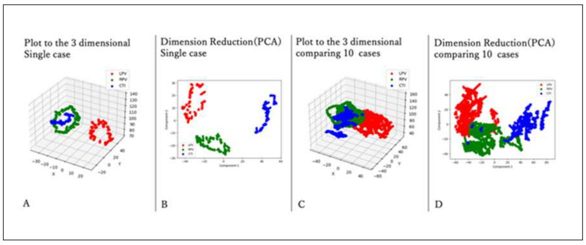

Figure 2. Visualizing 3-dimensional data extracted from the CARTO system for a single case [A] and its PCA dimension reduction [B]; comparing to the data of 10 cases [C] and its PCA dimension reduction [D].

Incorporating statistical data, a comprehensive dataset comprising 306,867 rows was created by integrating the data of 10 patients, as depicted in Fig. 3. This dataset represents a diverse range of cases, capturing nuances in ablation site characteristics across different patients. The large-scale dataset provides a robust foundation for the subsequent construction of a predictive model.

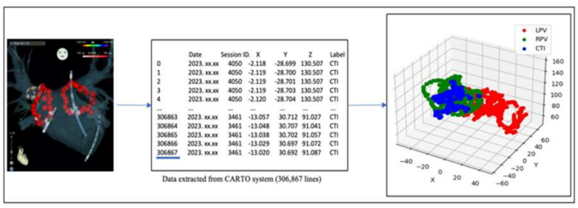

Figure 3. Data integration

To model the intricate relationships within the dataset, a supervised learning approach was employed. This involved training a predictive model to accurately forecast LPV, RPV, and CTI label data from the X, Y, and Z coordinate axes. The utilization of machine learning techniques not only facilitates the prediction of ablation site labels but also enables the extraction of valuable insights into the spatial dynamics of the cardiac anatomy.

Furthermore, the model construction process involved meticulous feature engineering to enhance the predictive capabilities. Features such as spatial relationships, proximity metrics, and temporal dynamics were considered to enrich the model's understanding of the underlying patterns within the ablation site dataset.

This comprehensive approach, combining advanced visualization techniques, statistical analysis, and machine learning methodologies, contributes to a deeper understanding of the complexities inherent in characterizing ablation sites. The findings derived from this extensive exploration lay the groundwork for improved clinical insights and advancements in the field of catheter ablation procedures.

V. RESULTS OF EXPERIMENT

In assessing prediction accuracy, all classifiers in the single-case dataset demonstrated exceptional performance, achieving an accuracy of 1.0. However, when transitioning to the mixed dataset of 10 cases, distinct variations in performance metrics were observed among the classifiers. Cross-validation involved testing each case individually as the test data while using the remaining 9 cases as training data. This process was repeated for each patient data from Data 1 to Data 10. The results are detailed as follows: k-NN (test score: 0.999, train score: 0.982, precision: 0.985, recall: 0.982, F-1 score: 0.983), GMM (test score: 0.981, train score: 0.983, precision: 0.986, recall: 0.983, F-1 score: 0.986), SGDClassifier (test score: 0.897, train score: 0.940, precision: 0.940, recall: 0.908, F-1 score: 0.907), and LinearSVC (test score: 0.796, train score: 0.889, precision: 0.851, recall: 0.796, F-1 score: 0.770), shown in Fig. 4.

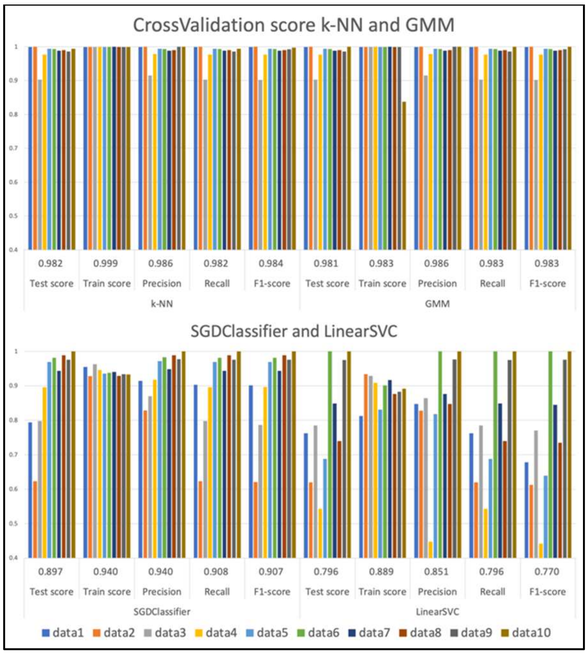

Figure 4. A comprehensive comparison of prediction accuracy, precision, recall, F-1 score among the k-NN, GMM, SGDClassifier, and LinearSVC.

Performance metrics were obtained through cross-validation, with the reported numbers representing the respective average values for each prediction. The results highlight the robustness of k-NN, showcasing consistently high and stable test scores across the board.

The exceptional accuracy achieved by all classifiers in the single-case dataset underscores the efficacy of the models in capturing and categorizing distinct ablation site patterns. However, when confronted with the increased complexity of the mixed dataset, subtle challenges in classification emerge, as evidenced by variations in performance metrics.

The GMM demonstrates strong predictive capabilities, with high test and train scores, emphasizing its adaptability to diverse patterns within the mixed dataset. Similarly, the KNN exhibits remarkable stability with consistently high test scores, making it a reliable choice for accurate predictions across varied cases.

In contrast, the SGDClassifier and LinearSVC, while still demonstrating respectable performance, show slightly diminished accuracy in the mixed dataset. These variations could be indicative of the challenges posed by overlapping RPV data observed in the principal component analysis results shown in Fig. 2.

The comprehensive comparison presented in Fig. 3 serves as a valuable guide for selecting appropriate classifiers based on the dataset characteristics. It provides insights into the relative strengths of each model in handling complex spatial patterns within the CARTO system's ablation site data. These findings contribute to the optimization of machine learning models for enhanced accuracy in predicting ablation site labels, thus advancing the application of such technologies in clinical settings.

VI. CONCLUSION

The results have indicated that nonlinear models consistently achieve high accuracy. Nonlinear models demonstrate notable adaptability to data, proving especially advantageous for discerning overlapping regions, as evidenced in this validation where their adaptability to overlapping sites with RPV was particularly beneficial. However, it is anticipated that with an increase in the number of mixed cases, the overlap area will also expand, indicating the need for new data to identify areas of overlap. In future endeavors to improve the accuracy of distinguishing overlapping sites, we plan to normalize the data, establish reference points, and implement further enhancements.

REFERENCES

[1] United nations, 2022. “Population”. https://www.un.org/en/global-iss ues/population

[2] Lutz, W., Sanderson, W. & Scherbov, S. “The coming acceleration of global population ageing”. Nature 451, 716–719 (2008). https://doi.org/10.1038/nature06516

[3] Eitaro Kodani, Hirotsugu Atarashi. “Prevalence of atrial fibrillation in Asia and the world”. Journal of Arrhythmia Volume 28, Issue 6 p. 330-337. https://doi.org/10.1016/j.joa.2012.07.001

[4] Haissaguerre Michel, et al. "Spontaneous initiation of atrial fibrillation by ectopic beats originating in the pulmonary veins." New England Journal of Medicine 339.10 (1998): 659-666. DOI: 10.1056/NEJM199809033391003

[5] Haissaguerre Michel, et al. "Electrophysiological breakthroughs from the left atrium to the pulmonary veins." Circulation 102.20 (2000): 2463-2465

[6] Philippe Maury, Benjamin Monteil, Lilian Marty, Alexandre Duparc, Pierre Mondoly, Anne Rollin. “Three-dimensional mapping in the electrophysiological laboratory”. https://doi.org/10.1016/j.acvd.2018.03.013

[7] Cover, T., & Hart, P. (1967). “Nearest neighbor pattern classification.”

[8] Bishop, C. M. (2006). “Pattern Recognition and Machine Learning.”

[9] Bottou, L., & Bousquet, O. (2008). “The tradeoffs of large scale learning.”

[10] Cortes, C., & Vapnik, V. (1995). “Support-Vector Networks.”